Virology 510 (2017) 175–184

Contents lists available at ScienceDirect

Virology

journal homepage: www.elsevier.com/locate/yviro

# Modeling the evolution of SIV sooty mangabey progenitor virus towards HIV-2 using humanized mice

Kimberly Schmitt[a,1], Dipu Mohan Kumar[a,1], James Curlin[a,1], Leila Remling-Mulder[a], Mark Stenglein[a], Shelby O'Connor[b], Preston Marx[c,d], Ramesh Akkina[a,*]

[a] Department of Microbiology, Immunology and Pathology, Colorado State University, Fort Collins, CO 80523, USA
[b] University of Wisconsin School of Medicine and Public Health, Madison, WI, USA
[c] Department of Tropical Medicine, School Public Health and Tropical Medicine, New Orleans, LA 70112, USA
[d] Tulane National Primate Research Center, Covington, LA 70433, USA

ARTICLE INFO

*Keywords:*
SIVsm evolution into HIV-2 lineage
Modeling SIV evolution into HIV in humanized mice
SIV pathogenesis in humanized mice
SIV genetic changes towards HIV-2
Origin of human pathogens in NHP
Viral adaptive changes and genetic evolution
Cross-species viral transmission

ABSTRACT

HIV-2 is thought to have originated from an SIV progenitor native to sooty mangabeys. To model the initial human transmission and understand the sequential viral evolution, humanized mice were infected with SIVsm and serially passaged for five generations. Productive infection was seen by week 3 during the initial challenge followed by chronic viremia and gradual $CD4^+$ T cell decline. Viral loads increased by the 5th generation resulting in more rapid $CD4^+$ T cell decline. Genetic analysis revealed several amino acid substitutions that were nonsynonymous and fixed in multiple hu-mice across each of the 5 generations in the *nef, env* and *rev* regions. The highest rate of substitution occurred in the *nef* and *env* regions and most were observed within the first two generations. These data demonstrated the utility of hu-mice in modeling the SIVsm transmission to the human and to evaluate its potential sequential evolution into a human pathogen of HIV-2 lineage.

## 1. Introduction

Cross-species transmission events have given rise to a number of human pathogens that have resulted in global pandemics/epidemics, including HIV-1 and HIV-2. While HIV-1 is responsible for most of the global AIDS pandemic, HIV-2 is also implicated as an important cause of the disease in a number of regions such as West Africa, Europe, India and the United States (Campbell-Yesufu and Gandhi, 2011). The origins of HIV-1 and HIV-2 from their ancestral SIV sources that eventually launched the AIDS epidemics during the 20th century remains an enigma awaiting experimental testing and explanation. Genomic evidence suggests that HIV-1 and HIV-2 evolved from cross-species transmission events involving chimpanzees and gorillas as well as sooty mangabeys, respectively (Chen et al., 1996; Hahn et al., 2000; Hirsch et al., 1989; Huet et al., 1990; Keele et al., 2006; Sharp et al., 1994; Van Heuverswyn et al., 2006). The fact that SIV has existed for millennia with the potential for zoonotic transmission, and that primates and humans have co-existed in West and Central Africa for thousands of years presents the question of what adaptive mutational changes brought about the emergence of the current HIV pandemic/epidemic (Fabre et al., 2009; Hirsch et al., 1989; Sharp et al., 1994; Worobey et al., 2010). Thus it is important to identify and elucidate the molecular changes in the progenitor SIV genomes during their transition from NHP viruses to human specific pathogens.

In order for SIV to infect a new primate species, the virus must be able to counteract numerous host restriction factors. These include: (1) APOBEC3G (apolipoprotein B mRNA-editing enzyme catalytic polypeptide-like 3G), which in the absence of Vif is packaged into the virion and deaminates cytidine residues during reverse transcription (Sheehy et al., 2002); (2) TRIM5α (tripartite motif 5α protein), which interferes with viral uncoating in a species-specific manner (Sayah et al., 2004; Stremlau et al., 2004); (3) SAMHD1, which acts by depleting the cellular dNTP pool available for reverse transcription (Berger et al., 2011; Goldstone et al., 2011; Hrecka et al., 2011); (4) SERINC3/5 (serine incorporator 3 and 5), acts by inhibiting the early stages of viral infection by impairing the penetration of the viral particle into the cytoplasm (Rosa et al., 2015; Usami et al., 2015); and (5) tetherin (also known as BST-2 and CD317), inhibits virus release by tethering virions to the plasma membrane (Le Tortorec and Neil, 2009; Neil et al., 2008). These host restriction factors act as barriers to cross-species infection, but can be overcome through adaptive mutations that alter how a protein interacts with the host restriction factor. APOBEC3G,

* Corresponding author.
*E-mail address:* akkina@colostate.edu (R. Akkina).
[1] The first three authors contributed equally.

http://dx.doi.org/10.1016/j.virol.2017.07.005
Received 23 May 2017; Received in revised form 3 July 2017; Accepted 5 July 2017
Available online 24 July 2017
0042-6822/ 

SAMHD1, SERINC3/5 and tetherin are all normally counteracted by Vif, Vpx/Vpr, Nef and Vpu/Nef; respectively. Env is utilized by HIV-2 in order to overcome the structural differences between simian and human tetherin (Goldstone et al., 2011; Jia et al., 2009; Kwak et al., 2010; Laguette et al., 2011; Le Tortorec and Neil, 2009; Neil et al., 2006, 2008; Usami et al., 2015; Zhang et al., 2009). A more complete understanding of how these SIV strains successfully evolved to overcome these restriction factors will provide insight into the evolutionary conflict that continues to occur between pathogenic retroviruses and their hosts.

An animal model that permits SIV infection of human cells *in vivo*, allowing for persistent viremia and long-term viral evolution, would be ideal to address many important questions surrounding the cross-species jump by SIV. The new generation of humanized mice, such as hu-HSC and BLT mice, that harbor a transplanted human immune system appear to be well suited for the task. Hu-HSC mice are prepared by engrafting human blood forming $CD34^+$ stem cells into immunodeficient neonatal mice (Akkina, 2013; Garcia and Freitas, 2012; Shultz et al., 2012). These hu-HSC mice have been shown to be susceptible to HIV-1 infection, sustain chronic viremia for as long as a year and display $CD4^+$ T cell loss that is the hallmark of HIV infection (Akkina, 2013; Berges et al., 2010). These mice have been previously used to study co-receptor switching from CCR5 to CXCR4, viral latency, HIV sexual transmission by vaginal and rectal routes and pre-exposure prophylaxis (PrEP) approaches (Akkina, 2013; Choudhary et al., 2012; Charlins et al., 2017; Garcia and Freitas, 2012; Neff et al., 2010). More recently, we also demonstrated the utility of the hu-HSC mouse model for understanding HIV-2 pathogenesis and testing ART (Hu et al., 2017). The presence of a broad spectrum human hematopoietic cells that encompass T cells, B cells, monocytes/macrophages and dendritic cells at various stages of development and viral susceptibility make these models particularly attractive to study human cell infectivity and the evolution of SIV primary isolates into HIVs in the context of cross-species transmission and pathogenic potential.

Several different hypotheses have emerged to explain how 13 independent SIV transmission events lead to the beginning of epidemic HIV strains. A leading hypothesis is that serial transmission of SIV in humans allowed for the accumulation of adaptive genetic changes in SIV leading to the emergence of epidemic HIV strains (Marx et al., 2001). Here, we sought to determine the evolution of SIVsm into HIV-2 using the hu-HSC mouse model to identify viral adaptive changes. To achieve this goal, we sequentially passaged SIVsm in hu-HSC mice and assessed viral loads, $CD4^+$ T cell depletion and genetic substitutions in each generation in comparison to the input stock virus. We observed hallmark characteristics of a pathogenic HIV infection in SIVsm infected hu-HSC mice, which included both an increase in plasma viral loads and the increasing loss of circulating $CD4^+$ T cells with each passage, which is indicative of increasing pathogenicity. Over the course of 5 passages, multiple nonsynonymous substitutions in the *nef*, *env* and *rev* genes were observed, with the *nef* and *env* regions displaying the highest rate of substitution. These data demonstrate that SIVsm can cross the species barrier and infect human immune cells *in vivo* and that this particular model can be used to tease-out specific adaptive substitutions required for viral evolution of SIV into a human pathogenic virus.

## 2. Results

### 2.1. SIVsmE041 causes productive infection and chronic viremia in hu-mice

To determine if a primary sooty mangabey SIV isolate can establish infection in hu-HSC mice, mice engrafted with HSC from two independent human donors were injected with SIVsmE041 by intraperitoneal route and serially passaged for a total of five generations (Figs. 1A and 1B). Plasma viral loads were monitored on a weekly basis by qRT-PCR. Viral infection was evident by week 2, with the viral loads increasing three logs by 70 days post-inoculation. The successful infection of hu-mice by SIVsm showed its ability to cause productive infection of human cells *in vivo*. We next proceeded to carry out serial passages of the virus in hu-mice. Viral loads peaked earlier during the 5th passage compared to the 1st passage followed by a gradual decline over the subsequent weeks, suggesting an increased fitness of the virus to infect its target cells with serial passage (Fig. 2A). No viral loads were detected as expected in control uninfected mice (data not shown).

### 2.2. SIVsmE041 infection leads to $CD4^+$ T cell depletion in hu-HSC mice

Previous studies have shown that a central hallmark of HIV infection in humans and hu-HSC mice is the depletion of $CD4^+$ T lymphocytes (Aldrovandi et al., 1993; Baenziger et al., 2006; Berges et al., 2006; Denton and Garcia, 2011). Peripheral blood samples collected bimonthly from SIVsm infected hu-HSC mice (Fig. 1) were assessed for circulating $CD4^+$ T cell levels using fluorophore conjugated antibodies for CD45, CD3 and CD4. Baseline $CD4^+$ T cell levels prior to infection were measured to be greater than 70% of all $CD3^+$ cells in each mouse. Mice from the first viral passage showed a gradual decline of circulating $CD4^+$ T cell levels, whereas the uninfected control mice did not show any marked $CD4^+$ T-cell depletion (Fig. 2B). In SIVsm infected mice, $CD4^+$ T-cell decline started within 10 days post-infection. In comparison, the rate of $CD4^+$ T cell depletion in passage 5 mice was more pronounced than in the earlier passages, suggesting increased pathogenicity of the virus to these cells (Fig. 2C). This is likely caused by the higher plasma viral loads observed in passage 5, and is similar to the pathology observed in end stage human AIDS (Fig. 2A). This data showed that SIVsm can establish viremia resulting in $CD4^+$ T cell depletion in the hu-HSC mouse model.

### 2.3. Genetic evolution of SIVsmE041 during sequential passages in hu-mice

Viral adaptation in response to host innate and/or adaptive immune pressures may select for certain genomic changes in the transmitted SIVsmE041 founder virus in humanized mice. Viral fitness can be impacted by a number of viral attributes such as the affinity for CD4 receptor binding or efficient cellular membrane fusion. Initial infection can be due to the existence of a low frequency variant in the Env region of the stock virus that eventually becomes selected as the dominant viral phenotype over time. Completely novel mutations that are not initially represented in the viral swarm can arise due to adaptive pressure to counteract the effects of host restriction factors like tetherin or APOBEC3 in the *nef*, *env* or *vif* regions. To assess genomic changes throughout the experiment and to search for possible signatures of viral adaptation, next-generation sequencing (NGS) was performed on the SIVsmE041 stock virus used to infect hu-HSC mice, as well as plasma RNA isolated from the infected animals from all 5 generations. Samples were collected at various time points ranging from 4 weeks to 6 months post-infection. We determined the consensus sequences of the stock virus and passaged viruses from each time point. The consensus sequence of the stock virus shared between 98.6 – 98.9% pairwise nucleotide identity in the coding region with the viruses from passage 1 – passage 5, which shared > 99.5% pairwise identity amongst themselves, indicating that the largest bottleneck may have occurred upon initial infection of human cells in the first passage (Fig. 3, Supplementary Table 1). We also calculated the frequency of all variants relative to the input virus with a frequency above 5%, and determined whether variants were synonymous or nonsynonymous. The stock virus, (p0), contained a number of variants with frequencies between 5% and 50%, as would be expected from a primary virus isolate (Fig. 3, Supplementary Table 1). Later generations contained

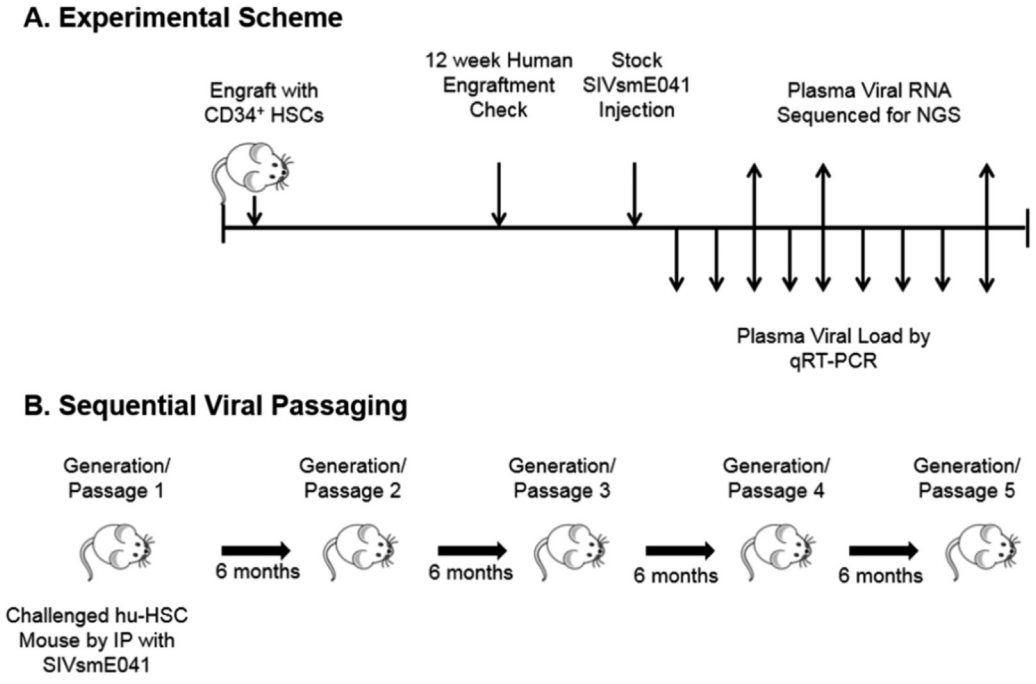


**Fig. 1.** SIVsmE041 infection of humanized mice. Schematic representation of the SIVsm infection and serial passage in hu-HSC mice.

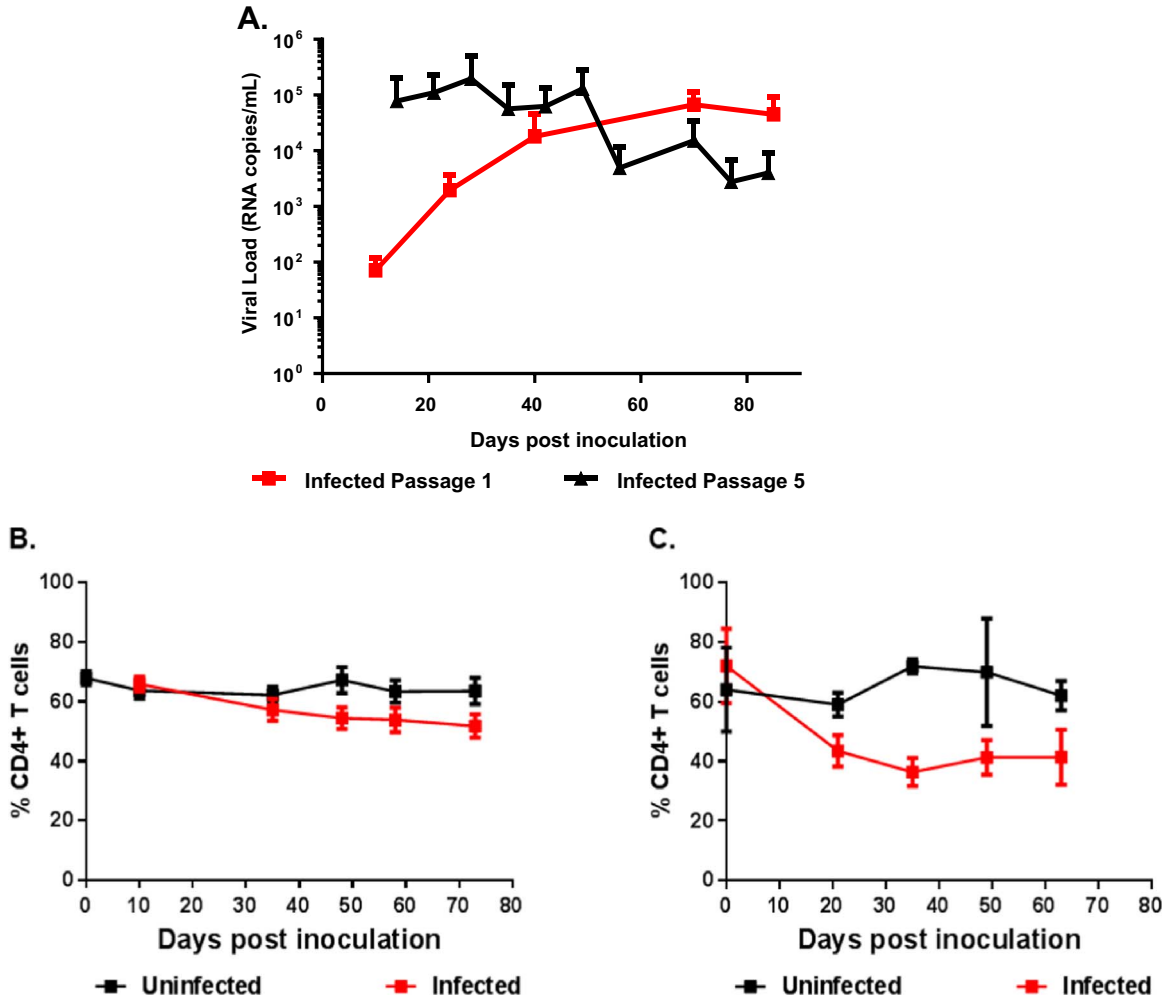


**Fig. 2.** SIVsmE041 infection leads to chronic viremia and a gradual decline of $CD4^+$ T cells in humanized mice. A) First and fifth generation plasma viral loads. Hu-HSC mice were infected via i/p route and viral loads were monitored by qRT-PCR on a weekly basis. No viral loads were detected in the uninfected control mice (data not shown). The percentage of circulating $CD4^+$ T cells relative to $CD3^+$ cells in the first (B) and fifth (C) generation consisting of SIVsm infected and uninfected hu-HSC mice. Statistically significant depletion was seen for both the first and fifth generation in infected mice relative to the uninfected mice (two-tailed Student's *t*-test, $p < 0.05$).

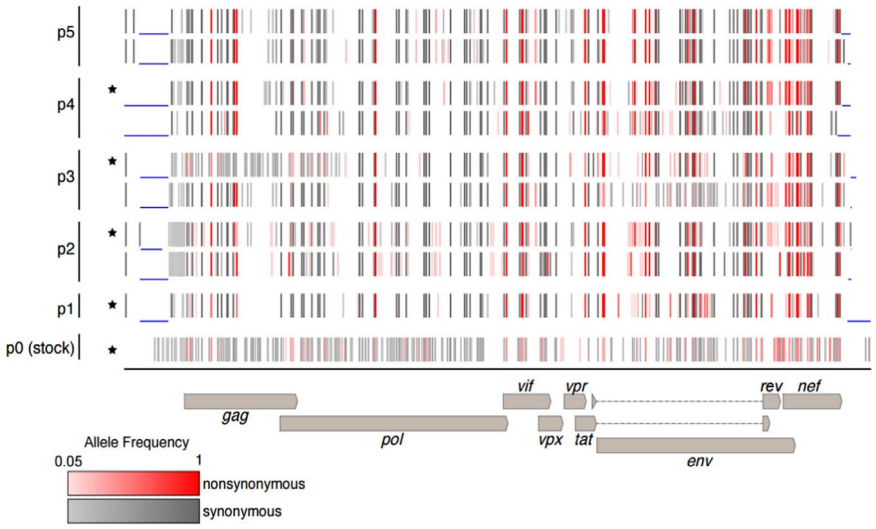


**Fig. 3.** Global variant analysis in virus populations during sequential passage. Frequencies of synonymous (grey) and non-synonymous (red) variants in the representative SIV populations were determined from sequencing data (see Section 4). Populations from two mice per passage are shown. Regions with lower than 20× sequencing coverage are indicated with blue lines, as well as the positions of the virus coding regions. Mice used as a source for inoculum for the subsequent passage are indicated with a (*).

**Table 1**
Amino Acid substitutions resulting from candidate adaptive mutations.

| Protein | Position | Stock consensus[a] | P5 variant[b] | Stock freq[c] | P1 freq[c] | P5 freq. rep. 1/2[d] | SIV fraction[e] | HIV-2 fraction[f] |
|---|---|---|---|---|---|---|---|---|
| Gag | 223 | P | Q | 0[g] | 0[g] | 1/1 | 0.00 | 0.00 |
| Gag | 233 | R | T | 0[g] | 0.26 | 1/1 | 0.02 | 0.04 |
| Gag | 482 | R | K | 0[g] | 0[g] | 0.56/0.58 | 0.84 | 0.65 |
| Vif | 136 | K | R | 0[g] | 0[g] | 0.57/0.68 | 0.29 | 0.07 |
| Vpr | 99 | G | S | 0[g] | 0[g] | 0.83/0.88 | 0.33 | 0.12 |
| Env | 158 | N | D | 0[g] | 0.06 | 1/1 | 0.03 | 0.07 |
| Env | 222 | R | Q | 0[g] | 0.13 | 1/1 | 0.87 | 0.16 |
| Env | 249 | N | D | 0[g] | 0.18 | 1/1 | 0.01 | 0.03 |
| Env | 393 | V | I | 0[g] | 0.28 | 1/1 | 0.01 | 0.04 |
| Rev | 34 | R | K | 0[g] | 0[g] | 0.9/0.76 | 0.00 | 0.01 |
| Env | 827 | E | G | 0[g] | 0[g] | 0.7/0.79 | 0.03 | 0.04 |
| Env | 829 | T | A | 0[g] | 0.15 | 1/0.98 | 0.35 | 0.86 |
| Nef | 92 | D | N | 0[g] | 0.09 | 1/0.99 | 0.02 | 0.03 |
| Nef | 94 | D | N | 0[g] | 0[g] | 0.59/0.44 | 0.03 | 0.12 |

[a] Consensus amino acid from stock virus sequencing dataset.
[b] Variant amino acid in p5 viruses.
[c] Frequency of variant mutation in stock sequencing dataset.
[d] Frequency of variant mutation in p5 replicate 1 and 2 sequencing datasets.
[e] Fraction of SIV sequences from HIV sequence compendium that contain the variant amino acid.
[f] Fraction of HIV-2 sequences from HIV sequence compendium that contain the variant amino acid.
[g] The 0 indicates below the limit of detection (5%) of our variant identification pipeline.

viral variants that ranged from 5% to 100% in allelic frequency. We searched for potentially adaptive variants according to several criteria. We reasoned that adaptive variants would be those that: (1) arose in the first passage and persisted at a high allelic frequency across subsequent passages, and/or (2) appeared in the first passage in multiple mice and increased in allelic frequency across the passages (Table 1, Supplementary Table 1; Fig. 4). Variants that increased in allelic frequency across multiple passages were found throughout the genome, with very few found in the *pol*, *vif*, *vpr* or *rev* genes. Conversely, *gag*, *env* and *nef* were found to have a higher frequency mutation with 3, 6 and 2 mutations, respectively (Fig. 4).

We also used the sequence alignments in the HIV Sequence Compendium (Foley et al., 2016) to assess whether the non-synonymous variants produce a more "HIV-2-like" virus. Specifically, we were interested in determining whether the variant changed the encoded amino acid to one present in a higher fraction of HIV-2 sequences than in SIVsm sequences. One mutation in particular, Env T829A, appeared at a relatively low rate in the first passage, but subsequently became the dominant variant as passages were carried forward. Additionally, while some SIV strains, such as SIVmac239, also contain this variant, it is frequently found amongst the HIV-2 subtypes A, B and H. (Table 1).

Patterns of variation were assessed for evidence of purifying (negative) or diversifying (positive) selection using SNPgenie (Nelson et al., 2015). The mean synonymous ($d_S$) and nonsynonymous ($d_N$) divergence from the reference sequence of the pooled NGS data was determined on a gene by gene basis (Fig. 5). Each gene showed varying degrees of divergence, with *nef* and *vif* showing the highest degree of nonsynonymous differences. In contrast, *vpx*, *gag* and *pol* all showed a markedly lower degree of nonsynonymous divergence relative to synonymous divergence, which indicates that these genes are undergoing a greater degree of purifying selection.

## 3. Discussion

Compelling evidence suggests that HIV-1 and HIV-2 arose through cross-species transmission events from their respective ancestral SIVs that are native to chimpanzees/gorillas and sooty mangabeys. However, the viral genetic evolution that occurs and is reflective of host adaptive changes is still not well understood. In this study, we

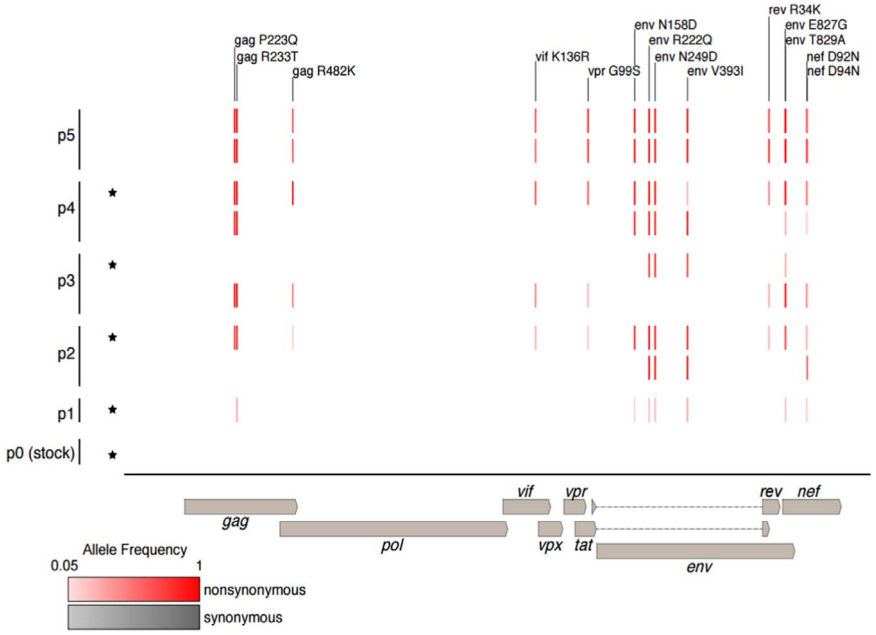


**Fig. 4.** Viral variants that increased in frequency between generations 1 and 5. Frequencies of nonsynonymous (red) and synonymous (grey) variants whose frequency increased by more than 0.5 between passage 1 and 5 in representative SIV populations were determined from sequencing data (see Section 4). Mice used as the source of inoculum for the subsequent passage are indicated with a (*).

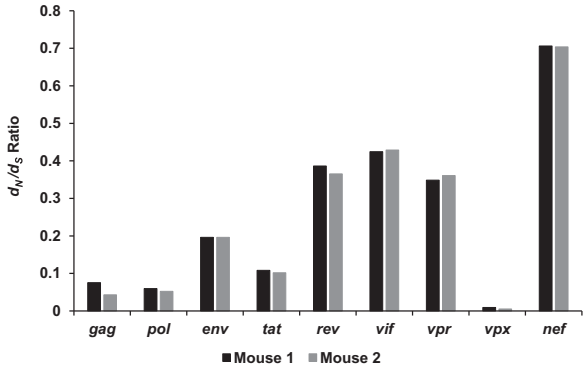


**Fig. 5.** The $d_N/d_S$ ratio of each gene from generation 5 calculated against the SIVsm reference sequence. The $d_N$ value was calculated via SNPgenie as the mean number of nonsynonymous differences from the reference per nonsynonymous site in the input sequence with the $d_S$ value being the mean number of synonymous differences from the reference per synonymous site in the input sequence. The *nef* and *vif* genes shows the greatest $d_N/d_S$ ratios in the genome, while *vpx, gag,* and *pol* all have drastically reduced ratios, suggesting that more divergent evolution is occurring in *nef* and *vif*.

used humanized mice to model SIVsm infection in human cells using a physiological setting *in vivo*, and performed serial passages of the virus to allow human adaptive changes, assessing both the phenotypic and genetic requirement for potential evolution into HIV-2. We used a primary isolate of SIVsmE041 stock virus, isolated from a 21 year old captive sooty mangabey. Whether or not this isolate is able to cause AIDS in an accelerated manner in a naïve young sooty mangabey remains to be determined. This virus was propagated in sooty mangabey PBMCs in order to infect hu-HSC mice and thus comprises a viral swarm. During our initial rounds of infection, we were able to successfully infect hu-HSC mice, which displayed viremia over the course of several months and thus confirmed that infection of human cells with a primary isolate of SIVsm is fully feasible and that persistent viremia could be sustained.

These infected mice also displayed $CD4^+$ T cell decline, recapitulating a key feature of human HIV infection. Comparison of viral growth and $CD4^+$ T cell loss kinetics between the first and fifth viral passages revealed that infection onset occurs at a faster rate, viral loads are higher and $CD4^+$ T cell loss is relatively more rapid during the fifth passage. This signifies enhanced viral adaptation and pathogenicity upon serial passage. This is consistent with the hypothesis that SIVsm has evolved gradually during sequential infections to become more pathogenic to humans (Marx et al., 2001). The data above collectively indicate successful evolution of SIVsm in becoming more fit to replicate *in vivo* in human cells and reflects the genetic changes in the parent virus during sequential passage. Accordingly, we analyzed the viral sequences from the first to the fifth passage virus by NGS and evaluated the sequence changes between these passages that encompass both synonymous and nonsynonymous mutations.

Among the important genetic changes that are predicted include the ability of the virus to gain entry into human cells efficiently and overcome host restriction factors. A number of host restriction factors, such as TRIM5α, APOBEC3G and tetherin, pose a potential species-specific barrier for viruses to mount a successful infection. Of these restriction factors, tetherin, a transmembrane host protein, appears to have the most significant impact during the evolution of HIV-1 and HIV-2 progenitors (Compton and Emerman, 2013; Simon et al., 2015). Most SIVs use the Nef protein to counteract tetherin by targeting its cytoplasmic domain, while HIV-1 uses the Vpu protein in a similar manner (Sharp and Hahn, 2011; Simon et al., 2015). Nef has a range of roles in HIV and SIV infection that include: downregulation of surface CD4 and MHC-1 expression, regulation of apoptosis, counteracting tetherin antagonism, altering the cellular state of activation and enhancing virion infectivity (Anderson et al., 1994; Arora et al., 2000; Atkins et al., 2008; Campbell et al., 2004; Chowers et al., 1994; Finkel et al., 1995; Garcia and Miller, 1991; Greenberg et al., 1998; Hua et al., 1997; Miller et al., 1994; Neil et al., 2008; Noviello et al., 2008; Sandstrom et al., 1996; Schwartz et al., 1996; Simmons et al., 2001; Wei et al., 2005; Wonderlich et al., 2008). Other SIVs and HIV-2 utilize their envelope proteins to target tetherin extracellular or cytoplasmic domains (Le Tortorec and Neil, 2009). In a *nef* deleted SIV mutant, compensatory changes were acquired by gp41 in order to counteract tetherin antagonism (Serra-Moreno et al., 2011). These varied anti-tetherin activities by lentiviruses appear to have evolved independently against host-specific selective pressures (Strebel, 2013).

We observed several nonsynonymous mutations in Nef and Env that became fixed in the population as seen in multiple mice across

each generation (Fig. 4; Supplementary Table 1). Consistently, we detected nonsynonymous mutations by passage 5 in Nef that corresponded to amino acid substitutions at positions R10H, K11R and H12R (Supplementary Table 1). These mutations occur in a region of *nef* that overlaps with *env* in a different reading frame. Additionally, these mutations are synonymous in the *env* reading frame and only appear to directly affect *nef*. However, the presence of these specific changes still warrants further investigation.

Homodimerization of Nef is important to create the PAK1/2 binding site that plays a crucial role in exerting the anti-apoptotic activity of Nef by the phosphorylation of Bad (Wolf et al., 2001). In HIV-1, this dimerization is stabilized by a salt-bridge formed between amino acid residues D123 and the dibasic R105-R106 motif (Kwak et al., 2010; Poe and Smithgall, 2009; Ye et al., 2004). One of the substitutions that became fixed by passage 5 in our study was the substitution of a lysine at position 105 into an arginine (K105R) which underscores the possible importance of this position in the host cell adaptation of SIV (Supplementary Table 1).

In SIVsm, Nef is used to counteract the action of tetherin, due to the absence of Vpu. However, HIV-2 alternatively utilizes Env to antagonize the human form of tetherin that contains a deleted cytoplasmic tail (Le Tortorec and Neil, 2009; Neil et al., 2008). Fixed mutations identified in the gp41 region of Env, E827G and T829A, may contribute to important adaptive changes (Fig. 4). Additionally, the Gag M30K/R substitution found in a previous study was observed in two mice from the second passage at very low allelic frequencies and was subsequently lost in future passages (data not shown) (Poe and Smithgall, 2009; Ye et al., 2004). This suggests that the Gag M30K/R substitution may not be critical for species-specific adaptation. However, more functional studies are needed to assess the importance of these mutations.

Further analysis of the genome as a whole, as well as on a gene by gene basis suggests that while certain regions are becoming more adapted, other components of the genome are much less tolerant of change. Using SNPgenie to assess the NGS data, $\pi_N$ represents the mean number of pairwise nonsynonymous differences per nonsynonymous site and $\pi_S$ is the same variable calculated for synonymous changes. These variables were able to be elucidated across the genome in a 9-codon sliding window analysis. The disparity between $\pi_N$ and $\pi_S$ values indicate how strong purifying selection is acting on a certain part of the genome (Nei and Gojobori, 1986). There were noticeable $\pi_S$ peaks that were present in each gene, which suggests that those regions may be subject to purifying selection, and are less likely to tolerate amino acid substitutions (Fig. 6). However, in several locations on the *vif* and *nef* genes, this trend is reversed and the $\pi_N$ peaks are much higher than $\pi_S$ at the same genomic locations. This could reflect positive (diversifying) selection and is consistent with the higher $d_N/d_s$ ratio associated with these genes (Fig. 6). The $\pi_N$ peaks do not cover the full length of each genome, but are instead representative of small 9 codon sliding windows of analysis. It is reasonable to conclude that while the genes as a whole favor purifying selection to prevent deleterious changes, individual regions within the genes may be more tolerant of variation and indeed may be the key drivers of viral adaptation into new hosts (Nelson and Hughes, 2015). These results provide a rational basis for follow-up studies to assess regions that control cross-species fitness.

A recent report by Yuan et al. utilized BLT hu-mice to assess infection with various chimpanzee SIVcpz strains to detect adaptive changes towards HIV-1. Interestingly, only two non-synonymous mutations in *env* were found in both SIVcpzMB897 and SIVcpzBF1167 (Yuan et al., 2016). This is likely due to the short 14-week period of evaluation during a single passage and that the whole genome was not analyzed by next-generation sequencing. Also, the chimpanzee strains used were grown from molecular clones representing homogeneous virus populations. In contrast, our study on the evolution of HIV-2 employed a primary SIVsm isolate, was serially passaged 5 times in hu-mice and the whole viral genomes were assessed for mutations on a global scale to detect notable viral genetic changes that are selected to become fixed during long term viral adaptation.

In summary, our results showed that SIVsm can infect hu-HSC mice causing chronic viremia leading to $CD4^+$ T cell decline. These properties are augmented between passage one and five indicating sequential viral adaptation. Sequence changes noted during viral adaptation may be indicative of increased fitness to the human host by passage 5; however, functional studies of these mutations are needed. While we recognize that the progeny virus from passage 5 has not fully evolved into HIV-2, it is likely that further passages are necessary and experiments are currently underway to evaluate this question. Nevertheless, our data demonstrates that SIVsm evolution in a human host can be modeled in hu-HSC mice and that key adaptation mutations will be identified and further characterized.

## 4. Materials and methods

### 4.1. Generation of humanized mice

Human fetal liver-derived CD34 cells were isolated, column purified (Miltenyi Biotec, San Diego, CA) and cultured as previously described (Akkina et al., 1994; Bai et al., 2000; Veselinovic et al., 2016). $CD34^+$ purity was assessed by flow cytometry. Neonatal Balb/c $Rag1^{-/-}\gamma c^{-/-}$ or Balb/c $Rag2^{-/-}\gamma c^{-/-}$ mice were preconditioned by irradiation at 350 rads and injected intrahepatically with 0.5–1 x $10^6$ human $CD34^+$ cells per mouse (Berges et al., 2008; Veselinovic et al., 2016). Transplanted mice were then screened at 10–12 weeks post-reconstitution for human cell engraftment. Peripheral blood was collected and the red blood cells were lysed using the Whole Blood Erythrocyte Lysing Kit and the manufacturer's instructions (R & D Systems, Minneapolis, MN). Fractioned white blood cells were stained with mouse anti-human CD45 FITC (eBioscience), CD3 PE (eBioscience) and CD4 PE/Cy5 (BD Pharmigen, San Jose, CA) for FACS analysis to confirm human cell engraftment (Berges et al., 2006; Veselinovic et al., 2016). Mice were maintained at the Colorado State University Painter Animal Center. The studies conducted in this publication have been reviewed and approved by the CSU Institutional Animal Care and Use Committee.

### 4.2. SIVsm primary isolate SIVsmE041

SM E041 was a male sooty mangabey born in January 1981 at the Yerkes Primate Research Center (YNPRC) for experimental leprosy infection and transferred in 1983 to the Tulane National Primate Research Center (TNPRC) (Gormus et al., 1995a, 1995b). E041 was infected with SIVsm by natural spread between group-housed mangabeys before leprosy experiments began at YNPRC and neither clinical nor histological evidence of leprosy was seen during 18 years of observation (Fultz et al., 1986; Ling et al., 2004; Murphey-Corb et al., 1986). SM E041 was 21 years old when euthanized with clinical signs of AIDS that included: high viral loads, low $CD4^+$ T-cell counts, SIV giant cell disease and B-cell lymphoma (Ling et al., 2004). The SIVsmE041 used in this study (Genbank accession HM059825.1) was propagated in sooty mangabey PBMC, making it a true primary isolate that is comprised of a population of closely related viruses. The tropism of this virus was determined to use the major co-receptor CCR5 (Ling et al., 2004).

### 4.3. SIVsmE041 infection of humanized mice and viral determination by qRT-PCR

Mice with high (> 70% $CD4^+$ T cells) human hematopoietic cell engraftment levels were used. At 16 weeks post engraftment, 200 μl of SIVsmE041 (TCID50, 811) was injected into five hu-HSC mice intraperitoneally (i/p). All humanized mice used in subsequent passages were inoculated with the same amount of virus using methodol-

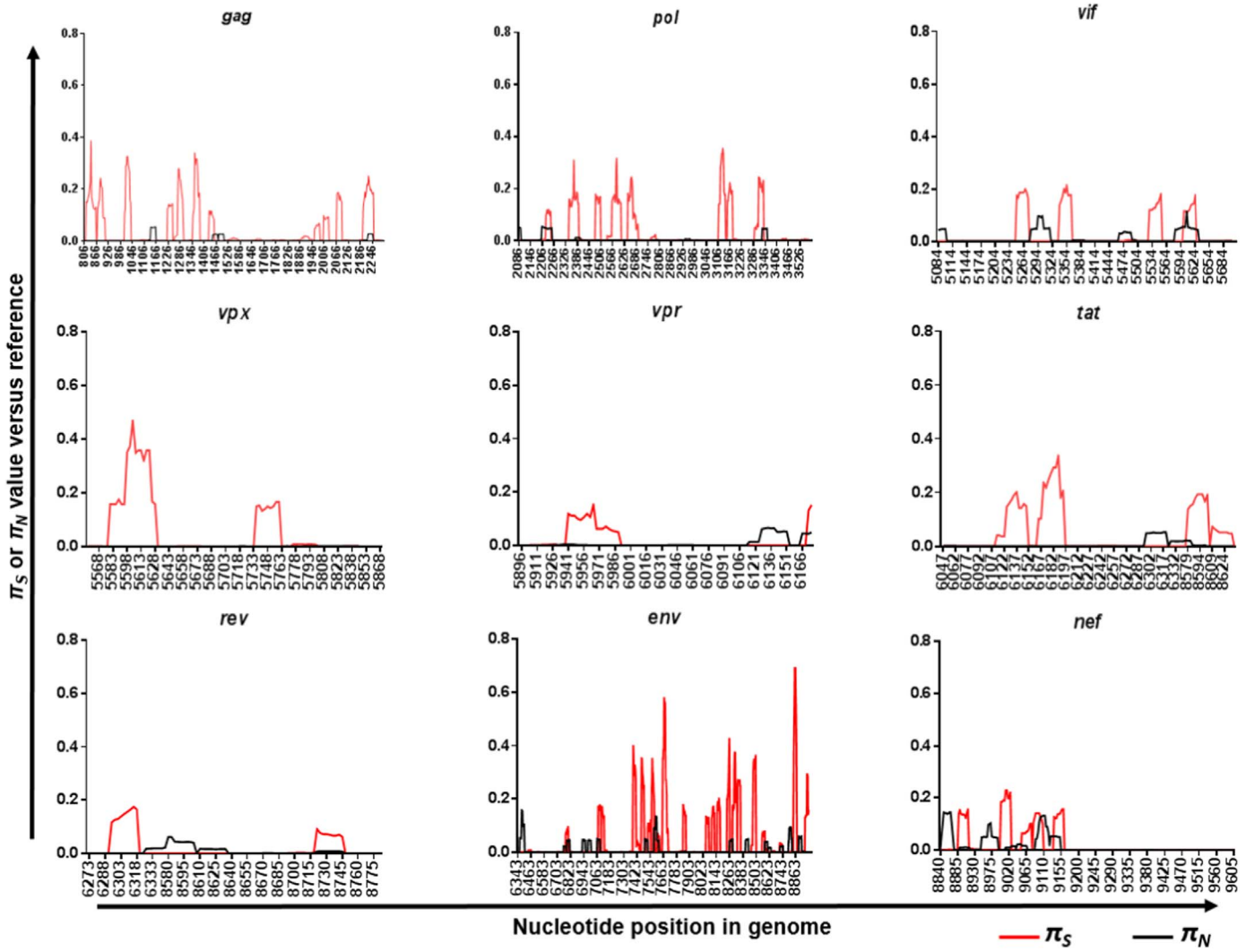


**Fig. 6.** 9-codon Sliding Window Analysis of Passage 5 Viral Genes. $\pi_N$ (black) and $\pi_S$ (red) of the passage 5 mice were calculated for each gene using a 9-codon sliding window analysis by SNPgenie. Multiple $\pi_S$ peaks were identified in each gene, with relatively low respective $\pi_N$ values, which indicate regions that may be crucial to the fitness of SIVsm. Alternatively, in other locations across multiple genes, particularly *vif* and *nef*, there are regions with markedly higher $\pi_N$ values relative to $\pi_S$, which is indicative of diversifying selection.

ogy as described above. Peripheral blood was collected weekly using non-heparinized capillary tubes to assess plasma viral load by tail vein puncture and transferred immediately to EDTA-containing vacutainer tubes (BD Biosciences, San Jose, CA). PBS was added to the plasma, with a final volume of 150 µl, and centrifuged at 400×*g* for 5 min. Plasma was removed and viral RNA was extracted from the plasma using the E.Z.N.A Viral RNA kit (OMEGA bio-tek, Norcross, GA). Viral loads were determined using the iScript One-Step RT-PCR kit with SYBR Green and the manufacturer's instructions (Bio Rad, Hercules, CA). Primers were designed based on a conserved region in SIVsmE041 *ltr* (GenBank accession number: HM059825.1). Forward (5′-CCACAAAGGGGATGTTATGGGG-3′) and reverse (5′-AACCTCCCAGGGCTCAATCT −3′) primers were used in a qRT-PCR reaction with the following cycling conditions: 50 °C for 10 min, 95 °C for 5 min, followed by 40 cycles of 95 °C for 15 s and 60 °C for 30 s in the Bio Rad C1000 Thermal Cycler with a CFX96 Real-Time System (Bio Rad, Hercules, CA). The standard curve was prepared using a series of 10-fold dilutions of viral SIVsmE041 *gag* at a known concentration. The sensitivity of this assay was 100 RNA copies per ml.

### 4.4. Determination of $CD4^+$ T cell levels

Flow cytometry was used to assess human cell engraftment levels in humanized SIVsm infected and uninfected mice. Peripheral blood was collected in heparinized capillary tubes by tail vein puncture bimonthly. 5 ul of FcγR-block (Jackson ImmunoResearch Laboratories, Inc. West Grove, PA) was added to the blood cell pellet and then stained with fluorophore conjugated hCD45-FITC (eBioscience), hCD3-PE (eBioscience) and hCD4-PE/CY5 (BD Pharmingen, San Jose, CA) for 30 min. Erythrocytes were lysed using a RBC lysing kit (BD sciences). After lysing, stained cells were washed twice with washing buffer (BD Sciences) and fixed in 1% paraformaldehyde. Stained cells were analyzed using BD Accuri C6 FACS analyzer. In order to measure $CD4^+$ T cell depletion in SIV infected mice, $CD3^+$ T cell levels were calculated as a ratio of the entire $CD45^+$ (lymphocyte common antigen marker) population. The $CD4^+$ T cell level was then determined based on the ratio of the entire $CD3^+$ T cell population. Engraftment levels of CD45, CD3 and CD4 were measured before infection as a control. $CD4^+$ T cell decline was assessed using a two-tailed Student's *t*-test ($< 0.05$) to compare the two groups of mice, infected and uninfected. All flow data was analyzed using the FlowJo software package (FlowJo LLC, Ashland, Oregon).

### 4.5. Illumina sequencing and analysis

Plasma viral RNA from week 4, 16 and 28 were extracted using the E.Z.N.A Viral RNA kit (Omega bio-tek, Norcross, GA) and amplified for 40 cycles using gene specific primers which span the full-length

**Table 2**
Primers utilized to generate amplicons for next-generation sequencing.

| Primer Location | Sequence |
|---|---|
| *gag* | Forward 5′-CGCTCTGTATTCAGTCGCTCTG-3′ |
| | Reverse 5′-GTCCCTCCTTTCCACAATTCCA-3′ |
| *gag/pol* | Forward 5′-GCTCAAGGGTCTGGGTATGAATC-3′ |
| | Reverse 5′-TGGAAAAATATGCATCACCTACA-3′ |
| *pol* | Forward 5′-CCTCCAACCAATCCATATAACACC-3′ |
| | Reverse 5′-GTCTCTGCCTCTGTCTGTCA-3′ |
| *pol* | Forward 5′-CTCAGTCAAGAACAAGAAGGGTG-3′ |
| | Reverse 5′-GCGATGTGAAGTTGGCACCATTATC-3′ |
| *pol/vif/vpx* | Forward 5′-GGACTTGGCAAATGGACTGT-3′ |
| | Reverse 5′-CTCGCCTACTGTTTCCTCTC-3′ |
| *vif/vpx/vpr/tat/rev* | Forward 5′-GACACCAGAGAAAGGATGGCTC-3′ |
| | Reverse 5′-GCTGATTCCCAAGACATCCCAT-3′ |
| *vpr/tat/rev/env* | Forward 5′-GGGTAGTAGAAGTTCTGGAGGAAG-3′ |
| | Reverse 5′-CTCTGTTTGTCCTTTCTTAACCCTG-3′ |
| *env* | Forward 5′-GGAACAACACAATGCTTGCCAG-3′ |
| | Reverse 5′-CTTCACTTCTCGGATAGCCCCT-3′ |
| *env* | Forward 5′-CCAGTCACCATTATGTCAGGGTTG-3′ |
| | Reverse 5′-CTGAACATAAACGGGAGGGGAAGA-3′ |
| *env/tat/rev/nef* | Forward 5′-GGATAGTGCAGCAACAGCAA-3′ |
| | Reverse 5′-TTCCATGCCAGCACCTCTCC-3′ |

genome of SIVsmE041 (Table 2). The amplicons from different primer sets were pooled together in equivalent amounts and subjected to next-generation sequencing (NGS) at the sequencing core facility at University of Wisconsin, Madison. All NGS sequencing samples were prepped using the Nextera XT DNA Library preparation kit and the manufacturer's instructions. The amplicon library was sequenced using Nextera XT kit and MiSeq Illumina desktop sequencer (Invitrogen). The sequence reads were obtained in FASTQ format and analyzed as described below.

### 4.6. Cell culture

Whole blood filter packs were obtained from the Garth Englund Blood Center of Fort Collins, CO. Mononuclear cells were isolated from human peripheral blood by Ficoll-Plaque density centrifugation. PBMCs were grown in RPMI media containing 10% fetal bovine serum (FBS), 2× antibiotic-antimycotic mix (Thermo Fischer Scientific) and 1% L-glutamine. PBMCs were activated for 24 h with PHA at a final concentration of 2 μg per ml and cultured in medium supplemented with 0.25 ng per ml of recombinant human IL-2 (R & D Systems, Inc., Minneapolis, MN & D R & D Systems, Inc., Minneapolis, MNystems, Inc., Minneapolis, MN). The GHOST (3) cell line positive for CD4, CXCR4 and CCR5 were cultured in DMEM with 10% FBS supplemented with 500 μg/ml G418, 100 μg/ml hygromycin and 1 μg/ml puromycin (Morner et al., 1999).

### 4.7. Viral propagation of SIVsm in vitro by co-culturing with activated human PBMC

SIVsm infected mice with the highest plasma viral titer were sacrificed at the end of the study and different tissues such as bone marrow, thymus, spleen, mesenteric lymph nodes and whole blood obtained by cardiac puncture were harvested. Single cell suspensions were made and leukocyte fraction isolated by Ficoll-Plaque density centrifugation. These cells were counted, plated at a density of 4–5 × $10^6$ cells/ml and activated using 2 μg/ml PHA and 0.25 μg/ml recombinant human IL-2 for 24 h. These cells were then co-cultured with 10 × $10^6$ freshly activated human PBMC from whole blood filter packs maintained in complete RPMI supplemented with 0.25 μg/ml recombinant human IL-2. Cell supernatant was harvested every third day and stored for use in future passages. Virus was quantified using qRT-PCR as mentioned above as well as by GHOST cell titration and flow cytometry. Five hu-HSC mice were then subsequently injected with 200 μl viral supernatant. This serial passage methodology was repeated for each consecutive generation.

### 4.8. Viral titration using GHOST cells

Ghost cells were seeded in a 48 well plate and infected with cell supernatant harvested from leukocyte/PBMC co-cultures in the presence of 8 μg/ml of polybrene (Sigma-Aldrich, St. Louis, MO). After 4 h, cells were centrifuged, washed and reseeded. The infected Ghost cells were harvested at 48 h post-infection, GFP expression assessed using flow cytometry and the viral titer calculated in order to begin the next generation of infection.

### 4.9. Calculation of variant frequencies in sequencing datasets

To calculate variant frequencies in sequencing datasets, we first removed the adapter sequences and low quality bases using the cutadapt software v1.9.1 (Martin, 2011). We then used cd-hit v4.6 to collapse PCR duplicated sequences (Li and Godzik, 2006). Reads were mapped to the stock virus consensus sequence using the bowtie2 software v2.2.5 (Langmead and Salzberg, 2012). Bowtie2 BAM format output was used as input to lofreq software v2.1.2 to call variants (Wilm et al., 2012). We required > 20 total aligned reads and > 5% frequency to call a variant.

### 4.10. Assessment of amino acid frequencies in HIV-2 and SIV database sequences

To assess whether amino acids were ‘more HIV-2-like’ or ‘more SIV-like’, we collected multiple sequence alignments for each viral protein from the 2016 HIV Sequence Compendium (Foley et al., 2016). These alignments consisted of ~68 HIV-2 sequences and ~ 30 SIVsm sequences. We created separate position probability matrices for the HIV-2 and the SIV sequences in each alignment that tabulated the estimated probability of each amino acid at each alignment position, using the position-based pseudo-count method (Henikoff and Henikoff, 1996). Positions with fewer than 75% gap characters were evaluated.

### 4.11. Determining the $d_N/d_S$ ratio of each gene from passage 5

Single Nucleotide Polymorphism (SNP) reports were generated as described above using lofreq. Using a FASTA file of the stock virus sequence obtained via NGS, a Gene Transfer Format (.gtf) file of the stock sequence with CDS information included as well as the SNP reports in VCF format (Format 2), SNPgenie (available at https://github.com/hugheslab/snpgenie) was used to calculate the $d_N$ and $d_S$ values relative to the stock virus sequence. Additionally, the nonsynonymous ($\pi_N$) and synonymous ($\pi_S$) nucleotide diversity were estimated by a 9-codon sliding window analysis with SNPgenie according to Nei and Gojobori's (1986) methodology (Nei and Gojobori, 1986).

## Acknowledgements

Work reported here was supported by NIH, USA grant RO1 AI12334 to R. A. This project was also supported in part by the National Center for Research Resources and the Office of Research Infrastructure Programs (ORIP) of the NIH through a grant OD011104 at the Tulane National Primate Research Center and an NIH grant P51OD011106 at the Wisconsin National Primate Research Center. We would like to thank the Tulane National Primate Research Center Virus Characterization, Isolation and Production Core for providing the SIVsmE041 viral stocks. We would also like to thank Sri Boddeda for help during the initial phases of these studies and Stephanie Feely for her technical assistance.

## Appendix A. Supplementary material

Supplementary data associated with this article can be found in the online version at http://dx.doi.org/10.1016/j.virol.2017.07.005.

## References


Akkina, R., 2013. New generation humanized mice for virus research: comparative aspects and future prospects. Virology 435 (1), 14–28.

Akkina, R.K., Rosenblatt, J.D., Campbell, A.G., Chen, I.S., Zack, J.A., 1994. Modeling human lymphoid precursor cell gene therapy in the SCID-hu mouse. Blood 84 (5), 1393–1398.

Aldrovandi, G.M., Feuer, G., Gao, L., Jamieson, B., Kristeva, M., Chen, I.S., Zack, J.A., 1993. The SCID-hu mouse as a model for HIV-1 infection. Nature 363 (6431), 732–736.

Anderson, S.J., Lenburg, M., Landau, N.R., Garcia, J.V., 1994. The cytoplasmic domain of CD4 is sufficient for its down-regulation from the cell surface by human immunodeficiency virus type 1 Nef. J. Virol. 68 (5), 3092–3101.

Arora, V.K., Molina, R.P., Foster, J.L., Blakemore, J.L., Chernoff, J., Fredericksen, B.L., Garcia, J.V., 2000. Lentivirus Nef specifically activates Pak2. J. Virol. 74 (23), 11081–11087.

Atkins, K.M., Thomas, L., Youker, R.T., Harriff, M.J., Pissani, F., You, H., Thomas, G., 2008. HIV-1 Nef binds PACS-2 to assemble a multikinase cascade that triggers major histocompatibility complex class I (MHC-I) down-regulation: analysis using short interfering RNA and knock-out mice. J. Biol. Chem. 283 (17), 11772–11784.

Baenziger, S., Tussiwand, R., Schlaepfer, E., Mazzucchelli, L., Heikenwalder, M., Kurrer, M.O., Behnke, S., Frey, J., Oxenius, A., Joller, H., Aguzzi, A., Manz, M.G., Speck, R.F., 2006. Disseminated and sustained HIV infection in CD34+ cord blood cell-transplanted Rag2-/-gamma c-/- mice. Proc. Natl. Acad. Sci. USA 103 (43), 15951–15956.

Bai, J., Gorantla, S., Banda, N., Cagnon, L., Rossi, J., Akkina, R., 2000. Characterization of anti-CCR5 ribozyme-transduced CD34+ hematopoietic progenitor cells in vitro and in a SCID-hu mouse model in vivo. Mol. Ther. 1 (3), 244–254.

Berger, A., Sommer, A.F., Zwarg, J., Hamdorf, M., Welzel, K., Esly, N., Panitz, S., Reuter, A., Ramos, I., Jatiani, A., Mulder, L.C., Fernandez-Sesma, A., Rutsch, F., Simon, V., Konig, R., Flory, E., 2011. SAMHD1-deficient CD14+ cells from individuals with Aicardi-Goutieres syndrome are highly susceptible to HIV-1 infection. PLoS Pathog. 7 (12), e1002425.

Berges, B.K., Akkina, S.R., Folkvord, J.M., Connick, E., Akkina, R., 2008. Mucosal transmission of R5 and X4 tropic HIV-1 via vaginal and rectal routes in humanized Rag2-/- gammac -/- (RAG-hu) mice. Virology 373 (2), 342–351.

Berges, B.K., Akkina, S.R., Remling, L., Akkina, R., 2010. Humanized Rag2(-/-) gammac(-/-) (RAG-hu) mice can sustain long-term chronic HIV-1 infection lasting more than a year. Virology 397 (1), 100–103.

Berges, B.K., Wheat, W.H., Palmer, B.E., Connick, E., Akkina, R., 2006. HIV-1 infection and CD4 T cell depletion in the humanized Rag2-/-gamma c-/- (RAG-hu) mouse model. Retrovirology 3, 76.

Campbell, E.M., Nunez, R., Hope, T.J., 2004. Disruption of the actin cytoskeleton can complement the ability of Nef to enhance human immunodeficiency virus type 1 infectivity. J. Virol. 78 (11), 5745–5755.

Campbell-Yesufu, O.T., Gandhi, R.T., 2011. Update on human immunodeficiency virus (HIV)-2 infection. Clin. Infect. Dis. 52 (6), 780–787.

Charlins, P., Schmitt, K., Remling-Mulder, L., Hogan, L.E., Hanhauser, E., Hobbs, K.S., Hecht, F., Deeks, S.G., Henrich, T.J., Akkina, R., 2017. A humanized mouse-based HIV-1 viral outgrowth assay with higher sensitivity than in vitro qVOA in detecting latently infected cells from individuals on ART with undetectable viral loads. Virology 507, 135–139.

Chen, Z., Telfier, P., Gettie, A., Reed, P., Zhang, L., Ho, D.D., Marx, P.A., 1996. Genetic characterization of new West African simian immunodeficiency virus SIVsm: geographic clustering of household-derived SIV strains with human immunodeficiency virus type 2 subtypes and genetically diverse viruses from a single feral sooty mangabey troop. J. Virol. 70 (6), 3617–3627.

Choudhary, S.K., Archin, N.M., Cheema, M., Dahl, N.P., Garcia, J.V., Margolis, D.M., 2012. Latent HIV-1 infection of resting CD4(+) T cells in the humanized Rag2(-)/(-) gammac(-)/(-) mouse. J. Virol. 86 (1), 114–120.

Chowers, M.Y., Spina, C.A., Kwoh, T.J., Fitch, N.J., Richman, D.D., Guatelli, J.C., 1994. Optimal infectivity in vitro of human immunodeficiency virus type 1 requires an intact nef gene. J. Virol. 68 (5), 2906–2914.

Compton, A.A., Emerman, M., 2013. Convergence and divergence in the evolution of the APOBEC3G-Vif interaction reveal ancient origins of simian immunodeficiency viruses. PLoS Pathog. 9 (1), e1003135.

Denton, P.W., Garcia, J.V., 2011. Humanized mouse models of HIV infection. AIDS Rev. 13 (3), 135–148.

Fabre, P.H., Rodrigues, A., Douzery, E.J., 2009. Patterns of macroevolution among Primates inferred from a supermatrix of mitochondrial and nuclear DNA. Mol. Phylogenet. Evol. 53 (3), 808–825.

Finkel, T.H., Tudor-Williams, G., Banda, N.K., Cotton, M.F., Curiel, T., Monks, C., Baba, T.W., Ruprecht, R.M., Kupfer, A., 1995. Apoptosis occurs predominantly in bystander cells and not in productively infected cells of HIV- and SIV-infected lymph nodes. Nat. Med. 1 (2), 129–134.

Foley, B., Leitner, T., Apetrei, C., Hahn, B., Mizrachi, I., Mullins, J., Rambaut, A., Wolinsky, S., and Korber, B. 2016. Reference for HIV sequence compendium: HIV sequence compendium 2016. Theoretical Biology and Biophysics, Publisher: Los Alamos National Laboratory, Los Alamos, New Mexico. LA-UR-16-25625.

Fultz, P.N., McClure, H.M., Anderson, D.C., Swenson, R.B., Anand, R., Srinivasan, A., 1986. Isolation of a T-lymphotropic retrovirus from naturally infected sooty mangabey monkeys (Cercocebus atys). Proc. Natl. Acad. Sci. USA 83 (14), 5286–5290.

Garcia, J.V., Miller, A.D., 1991. Serine phosphorylation-independent downregulation of cell-surface CD4 by nef. Nature 350 (6318), 508–511.

Garcia, S., Freitas, A.A., 2012. Humanized mice: current states and perspectives. Immunol. Lett. 146 (1–2), 1–7.

Goldstone, D.C., Ennis-Adeniran, V., Hedden, J.J., Groom, H.C., Rice, G.I., Christodoulou, E., Walker, P.A., Kelly, G., Haire, L.F., Yap, M.W., de Carvalho, L.P., Stoye, J.P., Crow, Y.J., Taylor, I.A., Webb, M., 2011. HIV-1 restriction factor SAMHD1 is a deoxynucleoside triphosphate triphosphohydrolase. Nature 480 (7377), 379–382.

Gormus, B.J., Xu, K., Baskin, G.B., Martin, L.N., Bohm, R.P., Blanchard, J.L., Mack, P.A., Ratterree, M.S., McClure, H.M., Meyers, W.M., et al., 1995a. Experimental leprosy in monkeys. I. Sooty mangabey monkeys: transmission, susceptibility, clinical and pathological findings. Lepr. Rev. 66 (2), 96–104.

Gormus, B.J., Xu, K., Cho, S.N., Baskin, G.B., Bohm, R.P., Martin, L.N., Blanchard, J.L., Mack, P.A., Ratterree, M.S., Meyers, W.M., et al., 1995b. Experimental leprosy in monkeys. II. Longitudinal serological observations in sooty mangabey monkeys. Lepr. Rev. 66 (2), 105–125.

Greenberg, M.E., Iafrate, A.J., Skowronski, J., 1998. The SH3 domain-binding surface and an acidic motif in HIV-1 Nef regulate trafficking of class I MHC complexes. EMBO J. 17 (10), 2777–2789.

Hahn, B.H., Shaw, G.M., De Cock, K.M., Sharp, P.M., 2000. AIDS as a zoonosis: scientific and public health implications. Science 287 (5453), 607–614.

Henikoff, J.G., Henikoff, S., 1996. Using substitution probabilities to improve position-specific scoring matrices. Comput. Appl. Biosci. 12 (2), 135–143.

Hirsch, V.M., Olmsted, R.A., Murphey-Corb, M., Purcell, R.H., Johnson, P.R., 1989. An African primate lentivirus (SIVsm) closely related to HIV-2. Nature 339 (6223), 389–392.

Hrecka, K., Hao, C., Gierszewska, M., Swanson, S.K., Kesik-Brodacka, M., Srivastava, S., Florens, L., Washburn, M.P., Skowronski, J., 2011. Vpx relieves inhibition of HIV-1 infection of macrophages mediated by the SAMHD1 protein. Nature 474 (7353), 658–661.

Hu, S., Neff, C.P., Kumar, D.M., Habu, Y., Akkina, S.R., Seki, T., Akkina, R., 2017. A humanized mouse model for HIV-2 infection and efficacy testing of a single-pill triple-drug combination anti-retroviral therapy. Virology 501, 115–118.

Hua, J., Blair, W., Truant, R., Cullen, B.R., 1997. Identification of regions in HIV-1 Nef required for efficient downregulation of cell surface CD4. Virology 231 (2), 231–238.

Huet, T., Cheynier, R., Meyerhans, A., Roelants, G., Wain-Hobson, S., 1990. Genetic organization of a chimpanzee lentivirus related to HIV-1. Nature 345 (6273), 356–359.

Jia, B., Serra-Moreno, R., Neidermyer, W., Rahmberg, A., Mackey, J., Fofana, I.B., Johnson, W.E., Westmoreland, S., Evans, D.T., 2009. Species-specific activity of SIV Nef and HIV-1 Vpu in overcoming restriction by tetherin/BST2. PLoS Pathog. 5 (5), e1000429.

Keele, B.F., Van Heuverswyn, F., Li, Y., Bailes, E., Takehisa, J., Santiago, M.L., Bibollet-Ruche, F., Chen, Y., Wain, L.V., Liegeois, F., Loul, S., Ngole, E.M., Bienvenue, Y., Delaporte, E., Brookfield, J.F., Sharp, P.M., Shaw, G.M., Peeters, M., Hahn, B.H., 2006. Chimpanzee reservoirs of pandemic and nonpandemic HIV-1. Science 313 (5786), 523–526.

Kwak, Y.T., Raney, A., Kuo, L.S., Denial, S.J., Temple, B.R., Garcia, J.V., Foster, J.L., 2010. Self-association of the Lentivirus protein, Nef. Retrovirology 7, 77.

Laguette, N., Sobhian, B., Casartelli, N., Ringeard, M., Chable-Bessia, C., Segeral, E., Yatim, A., Emiliani, S., Schwartz, O., Benkirane, M., 2011. SAMHD1 is the dendritic- and myeloid-cell-specific HIV-1 restriction factor counteracted by Vpx. Nature 474 (7353), 654–657.

Langmead, B., Salzberg, S.L., 2012. Fast gapped-read alignment with Bowtie 2. Nat. Methods 9 (4), 357–359.

Le Tortorec, A., Neil, S.J., 2009. Antagonism to and intracellular sequestration of human tetherin by the human immunodeficiency virus type 2 envelope glycoprotein. J. Virol. 83 (22), 11966–11978.

Li, W., Godzik, A., 2006. Cd-hit: a fast program for clustering and comparing large sets of protein or nucleotide sequences. Bioinformatics 22 (13), 1658–1659.

Ling, B., Apetrei, C., Pandrea, I., Veazey, R.S., Lackner, A.A., Gormus, B., Marx, P.A., 2004. Classic AIDS in a sooty mangabey after an 18-year natural infection. J. Virol. 78 (16), 8902–8908.

Martin, M., 2011. Cutadapt removes adapter sequences from high-throughput sequencing reads. EMBnet J. 17, 1.

Marx, P.A., Alcabes, P.G., Drucker, E., 2001. Serial human passage of simian immunodeficiency virus by unsterile injections and the emergence of epidemic human immunodeficiency virus in Africa. Philos. Trans. R. Soc. Lond. B Biol. Sci. 356 (1410), 911–920.

Miller, M.D., Warmerdam, M.T., Gaston, I., Greene, W.C., Feinberg, M.B., 1994. The human immunodeficiency virus-1 nef gene product: a positive factor for viral infection and replication in primary lymphocytes and macrophages. J. Exp. Med. 179 (1), 101–113.

Morner, A., Bjorndal, A., Albert, J., Kewalramani, V.N., Littman, D.R., Inoue, R., Thorstensson, R., Fenyo, E.M., Bjorling, E., 1999. Primary human immunodeficiency virus type 2 (HIV-2) isolates, like HIV-1 isolates, frequently use CCR5 but show promiscuity in coreceptor usage. J. Virol. 73 (3), 2343–2349.

Murphey-Corb, M., Martin, L.N., Rangan, S.R., Baskin, G.B., Gormus, B.J., Wolf, R.H., Andes, W.A., West, M., Montelaro, R.C., 1986. Isolation of an HTLV-III-related retrovirus from macaques with simian AIDS and its possible origin in asymptomatic mangabeys. Nature 321 (6068), 435–437.

Neff, C.P., Ndolo, T., Tandon, A., Habu, Y., Akkina, R., 2010. Oral pre-exposure prophylaxis by anti-retrovirals raltegravir and maraviroc protects against HIV-1 vaginal transmission in a humanized mouse model. PLoS One 5 (12), e15257.
Nei, M., Gojobori, T., 1986. Simple methods for estimating the numbers of synonymous and nonsynonymous nucleotide substitutions. Mol. Biol. Evol. 3 (5), 418–426.
Neil, S.J., Eastman, S.W., Jouvenet, N., Bieniasz, P.D., 2006. HIV-1 Vpu promotes release and prevents endocytosis of nascent retrovirus particles from the plasma membrane. PLoS Pathog. 2 (5), e39.
Neil, S.J., Zang, T., Bieniasz, P.D., 2008. Tetherin inhibits retrovirus release and is antagonized by HIV-1 Vpu. Nature 451 (7177), 425–430.
Nelson, C.W., Hughes, A.L., 2015. Within-host nucleotide diversity of virus populations: insights from next-generation sequencing. Infect. Genet. Evol. 30, 1–7.
Nelson, C.W., Moncla, L.H., Hughes, A.L., 2015. SNPGenie: estimating evolutionary parameters to detect natural selection using pooled next-generation sequencing data. Bioinformatics 31 (22), 3709–3711.
Noviello, C.M., Benichou, S., Guatelli, J.C., 2008. Cooperative binding of the class I major histocompatibility complex cytoplasmic domain and human immunodeficiency virus type 1 Nef to the endosomal AP-1 complex via its mu subunit. J. Virol. 82 (3), 1249–1258.
Poe, J.A., Smithgall, T.E., 2009. HIV-1 Nef dimerization is required for Nef-mediated receptor downregulation and viral replication. J. Mol. Biol. 394 (2), 329–342.
Rosa, A., Chande, A., Ziglio, S., De Sanctis, V., Bertorelli, R., Goh, S.L., McCauley, S.M., Nowosielska, A., Antonarakis, S.E., Luban, J., Santoni, F.A., Pizzato, M., 2015. HIV-1 Nef promotes infection by excluding SERINC5 from virion incorporation. Nature 526 (7572), 212–217.
Sandstrom, P.A., Pardi, D., Goldsmith, C.S., Chengying, D., Diamond, A.M., Folks, T.M., 1996. bc1-2 expression facilitates human immunodeficiency virus type-1 mediated cytopathic effects during acute spreading infections. J. Virol. 70 (7), 4617–4622.
Sayah, D.M., Sokolskaja, E., Berthoux, L., Luban, J., 2004. Cyclophilin A retrotransposition into TRIM5 explains owl monkey resistance to HIV-1. Nature 430 (6999), 569–573.
Schwartz, O., Marechal, V., Le Gall, S., Lemonnier, F., Heard, J.M., 1996. Endocytosis of major histocompatibility complex class I molecules is induced by the HIV-1 Nef protein. Nat. Med. 2 (3), 338–342.
Serra-Moreno, R., Jia, B., Breed, M., Alvarez, X., Evans, D.T., 2011. Compensatory changes in the cytoplasmic tail of gp41 confer resistance to tetherin/BST-2 in a pathogenic nef-deleted SIV. Cell Host Microbe 9 (1), 46–57.
Sharp, P.M., Robertson, D.L., Gao, F., Hahn, B.H., 1994. Origins and diversity of human immunodeficiency viruses. AIDS 8 (1), S27–S42.
Sharp, P.M., Hahn, B.H., 2011. Origins of HIV and the AIDS pandemic. Cold Spring Harb. Perspect. Med. 1 (1), a006841.
Sheehy, A.M., Gaddis, N.C., Choi, J.D., Malim, M.H., 2002. Isolation of a human gene that inhibits HIV-1 infection and is suppressed by the viral Vif protein. Nature 418 (6898), 646–650.
Shultz, L.D., Brehm, M.A., Garcia-Martinez, J.V., Greiner, D.L., 2012. Humanized mice for immune system investigation: progress, promise and challenges. Nat. Rev. Immunol. 12 (11), 786–798.
Simmons, A., Aluvihare, V., McMichael, A., 2001. Nef triggers a transcriptional program in T cells imitating single-signal T cell activation and inducing HIV virulence mediators. Immunity 14 (6), 763–777.
Simon, V., Bloch, N., Landau, N.R., 2015. Intrinsic host restrictions to HIV-1 and mechanisms of viral escape. Nat. Immunol. 16 (6), 546–553.
Strebel, K., 2013. HIV accessory proteins versus host restriction factors. Curr. Opin. Virol. 3 (6), 692–699.
Stremlau, M., Owens, C.M., Perron, M.J., Kiessling, M., Autissier, P., Sodroski, J., 2004. The cytoplasmic body component TRIM5alpha restricts HIV-1 infection in Old World monkeys. Nature 427 (6977), 848–853.
Usami, Y., Wu, Y., Gottlinger, H.G., 2015. SERINC3 and SERINC5 restrict HIV-1 infectivity and are counteracted by Nef. Nature 526 (7572), 218–223.
Van Heuverswyn, F., Li, Y., Neel, C., Bailes, E., Keele, B.F., Liu, W., Loul, S., Butel, C., Liegeois, F., Bienvenue, Y., Ngolle, E.M., Sharp, P.M., Shaw, G.M., Delaporte, E., Hahn, B.H., Peeters, M., 2006. Human immunodeficiency viruses: SIV infection in wild gorillas. Nature 444 (7116), 164.
Veselinovic, M., Charlins, P., Akkina, R., 2016. Modeling HIV-1 mucosal transmission and prevention in humanized mice. Methods Mol. Biol. 1354, 203–220.
Wei, B.L., Arora, V.K., Raney, A., Kuo, L.S., Xiao, G.H., O'Neill, E., Testa, J.R., Foster, J.L., Garcia, J.V., 2005. Activation of p21-activated kinase 2 by human immunodeficiency virus type 1 Nef induces merlin phosphorylation. J. Virol. 79 (23), 14976–14980.
Wilm, A., Aw, P.P., Bertrand, D., Yeo, G.H., Ong, S.H., Wong, C.H., Khor, C.C., Petric, R., Hibberd, M.L., Nagarajan, N., 2012. LoFreq: a sequence-quality aware, ultra-sensitive variant caller for uncovering cell-population heterogeneity from high-throughput sequencing datasets. Nucleic Acids Res. 40 (22), 11189–11201.
Wolf, D., Witte, V., Laffert, B., Blume, K., Stromer, E., Trapp, S., d'Aloja, P., Schurmann, A., Baur, A.S., 2001. HIV-1 Nef associated PAK and PI3-kinases stimulate Akt-independent Bad-phosphorylation to induce anti-apoptotic signals. Nat. Med. 7 (11), 1217–1224.
Wonderlich, E.R., Williams, M., Collins, K.L., 2008. The tyrosine binding pocket in the adaptor protein 1 (AP-1) mu1 subunit is necessary for Nef to recruit AP-1 to the major histocompatibility complex class I cytoplasmic tail. J. Biol. Chem. 283 (6), 3011–3022.
Worobey, M., Telfer, P., Souquiere, S., Hunter, M., Coleman, C.A., Metzger, M.J., Reed, P., Makuwa, M., Hearn, G., Honarvar, S., Roques, P., Apetrei, C., Kazanji, M., Marx, P.A., 2010. Island biogeography reveals the deep history of SIV. Science 329 (5998), 1487.
Ye, H., Choi, H.J., Poe, J., Smithgall, T.E., 2004. Oligomerization is required for HIV-1 Nef-induced activation of the Src family protein-tyrosine kinase, Hck. Biochemistry 43 (50), 15775–15784.
Yuan, Z., Kang, G., Ma, F., Lu, W., Fan, W., Fennessey, C.M., Keele, B.F., Li, Q., 2016. Recapitulating cross-species transmission of simian immunodeficiency virus SIVcpz to humans by using humanized BLT mice. J. Virol. 90 (17), 7728–7739.
Zhang, F., Wilson, S.J., Landford, W.C., Virgen, B., Gregory, D., Johnson, M.C., Munch, J., Kirchhoff, F., Bieniasz, P.D., Hatziioannou, T., 2009. Nef proteins from simian immunodeficiency viruses are tetherin antagonists. Cell Host Microbe 6 (1), 54–67.